



Size- and composition-induced band-gap change of nanostructured compound of II–VI semiconductors

Y. Wang^{a,c}, G. Ouyang^{b,c,*}, L.L. Wang^a, L.M. Tang^a, D.S. Tang^b, Chang Q. Sun^{c,*}

^aSchool of Physics and Microelectronics Science, Hunan University, Changsha 410082, China

^bKey Laboratory of Low-Dimensional Quantum Structures and Quantum Control of Ministry of Education, and Department of Physics, Hunan Normal University, Changsha 410081, China

^cSchool of Electrical and Electronic Engineering, Nanyang Technological University, Singapore 639798, Singapore

ARTICLE INFO

Article history:

Received 4 July 2008

In final form 22 August 2008

Available online 27 August 2008

ABSTRACT

We have investigated the joint effect of size- and composition-induced band-gap change of semiconductive nanocompounds from the recently developed bond-order-length-strength (BOLS) correlation mechanism using the approach of local bond average (LBA). An analytical solution has been developed to connect the band-gap energy with the bonding identities of the nanocompounds. Agreement between the model predictions with the available experimental measurements of band-gap change of II–VI semiconductor nanocompounds showed that both the particle size and the composition with alloying effect can be used as factors tuning the band-gap energy, suggesting an effective way to realize the desirable properties of semiconductive nanocompounds.

© 2008 Elsevier B.V. All rights reserved.

1. Introduction

The semiconductive nanocompounds have been attracted considerable attention for decades due to their unique physical and chemical properties, which make them as the ideal advanced functional materials for nanodevices [1–3]. Due to the band-gap of semiconductor materials playing a fundamental role in electrical and optical properties, it is important and necessary to study on the band-gap change in order to gain a better understanding for their relevant properties. Up to date, the band-gap of pure nanoparticles has been extensively explored with size in detail [4–8]. It can be observed that the band-gap displays blue shift with decreasing the size because of surface skin quantum trapping. In most cases, just tuning the size can obtain the demanded band-gap energy. However, to meet wider band-gap, it costs thermal stability and luminescence efficiency of nanometer scale system with decreasing the size, especially the size is less than 2–3 nm [9–11]. Fortunately, nanosemiconductor alloys not only have the basic optical properties as pure semiconductor nanoparticles but also have their own superiorities such as high luminescence, much more stability and a single system with multiple characteristic. That is why the study of alloy is beginning to rise from experimentally [12–21] to theoretically. A large number of experiments have been reported that the band-gap of homogeneous alloy $E_g(x, D)$ express the nonlinear function with composition x (the molar ratio).

Several models with regard to composition-induced band-gap change of homogeneous nanostructure alloys have been developed, such as [10,11,19,20]:

$$E_g(x, D) = \begin{cases} xE_g(1, D) + (1-x)E_g(0, D) - bx(1-x) & \text{(empirical)} \\ xE_g(1, D) + (1-x)E_g(0, D) & \text{(Vegard et al.)} \\ 1/(\frac{x}{E_g(1, D)} + \frac{1-x}{E_g(0, D)}) & \text{(Fox)} \\ xE_g(1, D) + (1-x)E_g(0, D) + \Omega(x, D)x(1-x) & \text{(Zhu et al.)} \end{cases} \quad (1)$$

where the coefficient b represents the nonlinear effect resulting from the anisotropic nature of binding, which is difficult to measure in experiment. Although no adjustable parameters are used in Vegard's law and Fox's model, the former does not describe well the relationship between the band-gap and the composition, and the latter could not reproduce the measured data reasonably if the atomic interaction energy of the alloy components is strong. Strikingly, Zhu et al. [10] recently proposed the model based on Vegard's law which performs better than the others as mentioned above because they have considered the size-dependent atomic interaction bond energy $\Omega(x, \infty)$. However, among these theoretical methods above, the atomistic origin between the band-gap and the bonding identities of nanocompounds is not properly addressed. Therefore, for this reason, in this contribution, we present an atomistic insight into the size dependence of the composition-induced band-gap change of II–VI semiconductor nanocompound based on the recently developed bond-order-length-strength (BOLS) correlation mechanism using the approach of local bond average (LBA) [6,22]. Our theoretical results revealed the composition-dependence band-gap yields a downward bowing behavior arising from

* Corresponding authors. Address: School of Electrical and Electronic Engineering, Nanyang Technological University, Singapore 639798, Singapore (G. Ouyang).

E-mail addresses: gangouy@hunnu.edu.cn (G. Ouyang), ecqsun@ntu.edu.sg (C.Q. Sun).

inter-atomic interaction of alloy components and the size-dependent band-gap expansion displays a rising trend because of the broken bond-induced lattice strain and quantum trapping in the relaxed surface region. It is also found that the size and composition with alloy effect can tune the band-gap energy, which suggests an effective way to reach the desirable electrical and optical properties.

2. Principle

The BOLS correlation mechanism [6], extending from the Goldschmidt's and Pauling's considerations [23,24] to energy domain, indicates the physical origin of the shape- and size-dependence of bond length, bond nature and bond strength of nanosolids. It elucidates well that band-gap expansion originates from the coordination-imperfect-induced bond contraction spontaneously and the associated with bond energy rising at the curved surface of a nanosolid. According to the nearly-free-electron method, the width of the gap is equal to twice the Fourier component of the crystal potential, that is $E_g = 2|\int V(N, r)e^{ik \cdot r} dr|$, where the $V(N, r)$ is the crystal potential, k is the wave vector describing the nearly-free-electrons. Taken the contributions from the outer most relaxed region into consideration, the potential of Hamiltonian of a nanosolid follows the relation [6], i.e., $V(D) = V_{\text{atom}}(r) + V_{\text{cry}}(r)(1 + \delta_{\text{surf}})$, where $V_{\text{atom}}(r)$ is the intra-atomic trapping potential, defining the core-level position of an isolated atom; $V_{\text{cry}}(r)$ is the crystal potential of an extended solid, that sums the energies of inter-atomic binding potential in the particular site r over the entire solid, δ_{surf} describes the surface perturbation to the crystal binding energy independent of the particular form of the inter-atomic potential. Accordingly, the corresponding band-gap of nanosolids due to the overall potential in the Hamiltonian of an extended solid is given as follows [6]:

$$E_g(D) = E_g(\infty) + E_g(\infty) \cdot \delta_{\text{surf}} = (1 + \delta_{\text{surf}})E_g(\infty)$$

$$\delta_{\text{surf}} = \sum_{i \leq 3} \gamma_i (c_i^{-m} - 1)$$

$$\gamma_i \cong \frac{\tau \cdot c_i}{K}$$

$$c_i = 2 / \{1 + \exp[(12 - z_i)/(8z_i)]\}$$
(2)

where γ_i is the surface/volume ratio of different dimensionality [τ is the dimensionality of a thin plate ($\tau = 1$), a rod ($\tau = 2$) and a spherical dot ($\tau = 3$)]; c_i is the bond contraction coefficient that formulated Goldschmidt's notation [23]; $c_i^{-m} = \varepsilon_i/\varepsilon_0$ represents the energy change with the reduced bond length; d_0 is the bond length of atom in bulk; $K = D/2d_0$ that is the number of atoms lined along the radius of a nanosolid; subscript i denotes the specific i th atom of concern, which is counted from the outermost atomic layer to the center of the solid; z_i is the effective CN of an atom in the outermost atomic layer ($z_1 = 4(1 - 0.75/K)$, $z_2 = 6$ and $z_3 = 12$); ∞ denotes the bulk; the coefficient m is an adjustable parameter varying with the nature of the chemical bond. Note that the value of bond nature m is determined according to experimental results, not being freely adjustable. It is evident that the band-gap energy depends on both bond contraction and surface/volume ratio.

With regard to the bulk semiconductor alloy ($A_xB_{1-x}C$), the band-gap energy ($E_g(x, \infty)$) is contributed from the separate parts of the pure semiconductor compounds AC and BC with composition and the averaged single bond energy $E_0(\infty)$ describing atomic interaction bond energy between two components of semiconductor alloy. It can be expressed as [10,25,26]:

$$E_g(x, \infty) = x \cdot E_g(AC, \infty) + (1 - x) \cdot E_g(BC, \infty) + x(1 - x) \cdot E_0(\infty)$$
(3)

When semiconductor alloy comes to the nanometer size, the value $E_g(x, D)$ is also primarily determined by the above factors, which all depend on size. Through the BOLS mechanism, it is easy to obtain $E_g(\alpha, D)$ and $E_i(D)$ from the bulk counterparts as follows:

$E_g(\alpha, D) = (1 + \delta_{\text{surf}})E_g(\alpha, \infty)$ and $E_i(D) = (1 + \delta_{\text{surf}})E_0(\infty)$, where α denotes semiconductor compound AC or BC. $E_i(D)$ is the size-dependent averaged single bond energy of alloy. Consequently, based on the considerations above, the analytic $E_g(x, D)$ function of nanosemiconductor alloy is described as:

$$E_g(x, D) = (1 + \delta_{\text{surf}})[x \cdot E_g(AC, \infty) + (1 - x) \cdot E_g(BC, \infty) + x(1 - x) \cdot E_0(\infty)]$$
(4)

3. Results and discussion

To investigate the impacts of size and composition on band-gap energy of bulk and nanosemiconductor compounds, we have compared with the band-gap of them among the theoretical methods in terms of Eq. (3) or Eq. (4) and the available experimental results. The calculation parameters are given in Table 1. Fig. 1 shows the

Table 1
Parameters used in calculation of experimental observation

	E_g (bulk) (eV)	d_0 (bulk) (nm)	m
ZnS	3.6 [28]	0.234 [32]	4.0 [35]
ZnSe	2.7 [29]	0.245 [29]	2.1 [36]
CdS	2.53 [30]	0.247 [33]	3.05 [19]
CdSe	1.74 [31]	0.268 [34]	1.7 [37]
CdTe	1.44 [19]	0.286 [19]	4.0 [19]

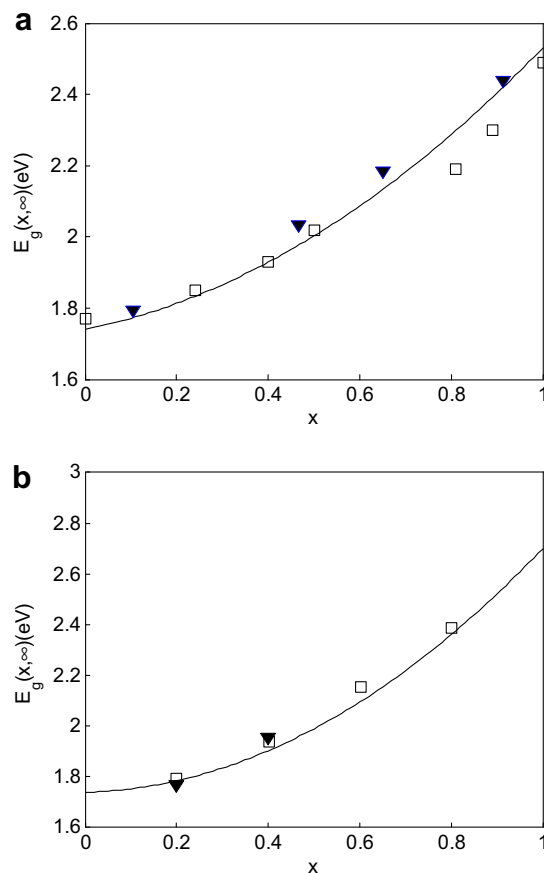


Fig. 1. Agreement between predictions (solid line) and experimental measurements (symbols) of the composition dependence of band-gap in bulk alloy. (a) $\text{CdS}_x\text{Se}_{1-x}$, (b) $\text{Zn}_x\text{Cd}_{1-x}\text{Se}$, (c) $\text{Zn}_x\text{Cd}_{1-x}\text{S}$ and (d) $\text{CdTe}_x\text{Se}_{1-x}$. The symbols are cited from: \square [21] and \blacktriangledown [19] in (a); \square [13] and \blacktriangledown [12] in (b); \square [14] in (c) and \square [15] in (d). The $E_0(\infty)$ [10] values of $\text{CdS}_x\text{Se}_{1-x}$, $\text{Zn}_x\text{Cd}_{1-x}\text{Se}$, $\text{Zn}_x\text{Cd}_{1-x}\text{S}$ and $\text{CdTe}_x\text{Se}_{1-x}$ are -0.53 eV, -0.92 eV, -1.01 eV and -0.83 eV.

theoretical predictions and the experimental measurements for the $E_g(x, \infty)$ function of bulk semiconductor alloys ($\text{CdS}_x\text{Se}_{1-x}$, $\text{Zn}_x\text{Cd}_{1-x}\text{Se}$, $\text{Zn}_x\text{Cd}_{1-x}\text{S}$ and $\text{CdTe}_x\text{Se}_{1-x}$). Clearly, the band-gap $E_g(x, \infty)$ slides obviously from bulk band-gap of one pure component at one side ($x = 0$) to that of another pure component at the other side ($x = 1$), which results from the alloying formation via the intermixing the wider band-gap with the narrower band-gap. Whether $E_g(x, \infty)$ appears blue shift or red shift is ascribed to the band-gap that is narrower or wider at $x = 0$ side. If we consider the impact of the constituents on the alloy band gap separately, there should be a linear relation between the band-gap energy and the composition. However, the nonlinear curve displays a downward bowing behavior due to the effect of the alloying effect. Noted that the value $E_0(\infty)$ of the semiconductor alloy is taken for simplicity [10,27], Figs. 2 and 3 show the band-gap energy behavior of homogeneous alloyed semiconductor nanodots and nanowires with varying composition and maintaining a small size in terms of BOLS mechanism. Apparently, the band-gap energy $E_g(x, D)$ of nanodots and nanowires has similar behavior to the corresponding bulk counterparts.

Fig. 4 shows the size-dependent band-gap expansion in semiconductor nanodots and nanowires with fixed composition. The inset in Fig. 4a displays the small-size part of the band-gap and the corresponding fitting curve from 2 nm to 10 nm. As shown in the figure, the band-gap energy firstly drops rapidly and then declines slowly with increasing the size despite of nanodots or nanowires,

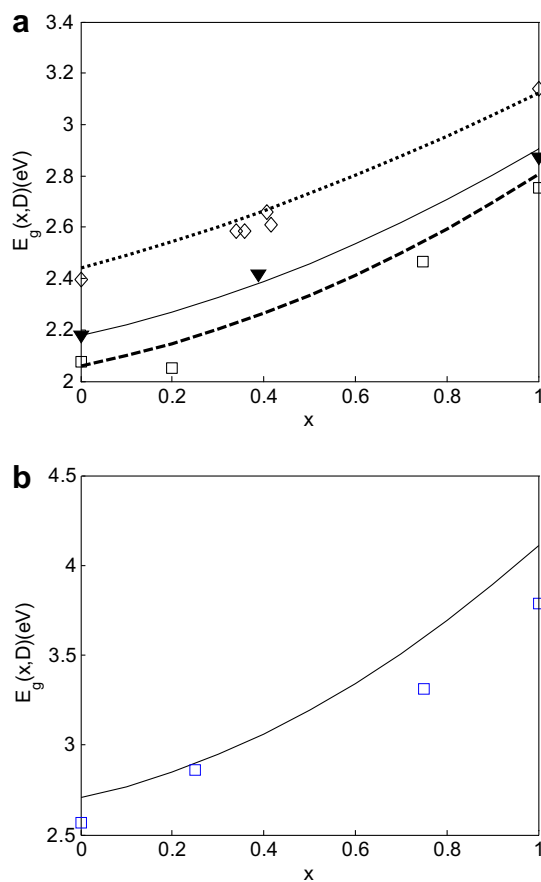


Fig. 2. In (a), the dotted, solid and dashed curves show the predictions of composition-dependent band-gap $E_g(x, D)$ of $\text{CdS}_x\text{Se}_{1-x}$ nanodots with different size. The corresponding sizes of the shown symbols are: 2.8 nm (\diamond [19]), 4.3 nm (\blacktriangledown [19]) and 5.8 nm (\square [19]) and the bulk band energy is -0.53 eV. In (b) and (c), comparison of the predictions with the measurements on the composition dependence $E_g(x, D)$ of semiconductor nanodots with maintaining size D . The corresponding diameter D and $E_0(\infty)$ [9] values are: $\text{Zn}_x\text{Cd}_{1-x}\text{S}$ (9 nm, -1.01 eV) [14] and $\text{Zn}_x\text{Cd}_{1-x}\text{Se}$ (10 nm, -0.92 eV) [20], respectively.

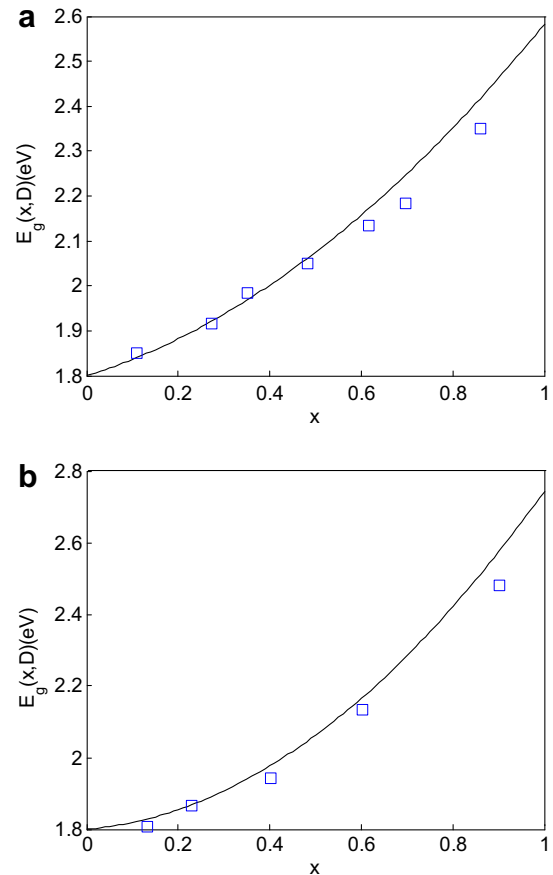


Fig. 3. Agreement between predictions (solid line) and experimental measurements (symbols) of the composition dependence $E_g(x, D)$ of semiconductor nanowires with diameter 20 nm: (a) $\text{CdS}_x\text{Se}_{1-x}$ [17] and (b) $\text{Zn}_x\text{Cd}_{1-x}\text{Se}$ [16]. The $E_0(\infty)$ [10] values of $\text{CdS}_x\text{Se}_{1-x}$ and $\text{Zn}_x\text{Cd}_{1-x}\text{Se}$ are -0.5 eV and -0.35 eV. The symbols shown are corresponding experimental results.

which is similar to that of pure nanostructures [6,8]. The reason is the variation of surface/volume ratio and the relaxation effects of surface atoms. Detailedly, the band-gap change of alloy with size and composition in $\text{Zn}_x\text{Cd}_{1-x}\text{Se}$ nanodots is shown in Fig. 5. It is clearly seen that the band-gap is inversely proportional to the size and the composition, which is also supported by Figs. 1–4. Interestingly, both the size and the composition can tune the band-gap energy of nanocompounds. In particular, the composition-tunable band-gap may be a better way for wider band-gap materials. Taken the Fig. 2a as an example, the band-gap of $\text{CdS}_x\text{Se}_{1-x}$ expands less than 0.5 eV from 5.8 nm to 2.8 nm with maintaining x , while it likely expands at least 0.5 eV with altering x not changing the size D . Though both ways can tune band-gap energy of materials, in order to meet the same desirable band-gap energy of nanocompounds, adjusting size will lead to system instability and hard fabrication while modulating composition can avoid these drawbacks. Evidently, it is a better way to obtain the wider band-gap materials by tuning the composition compared with the size of nanocompounds.

4. Conclusion

In summary, the band-gap energy change of nanocompounds is well addressed based on the BOLS correlation mechanism, which enable us to understand the composition- and size-dependent band-gap energy in nanostructure alloy involving CN-imperfection-enhanced bond strength at a surface with no assumption or freely adjustable variables. The results reveal the variable trend

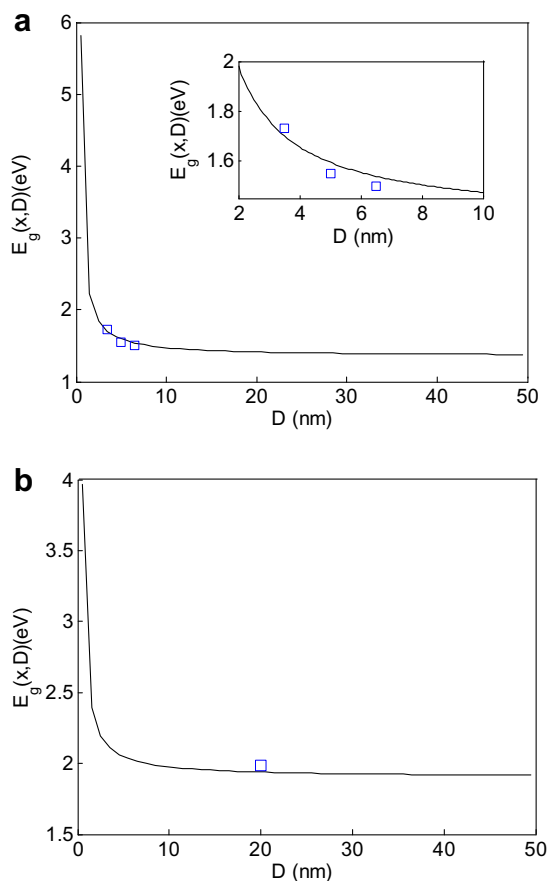


Fig. 4. Agreement between prediction (solid lines) and experimental measurements (symbols) of the size- and shape- dependence of band-gap of (a) $\text{CdSe}_x\text{Te}_{1-x}$ [15] nanodots with $x = 0.66$, $E_0(\infty)$ [10] is -0.83 eV. The small-size part of the same band-gap energy and corresponding fitting curve are shown in the inset; (b) $\text{CdS}_x\text{Se}_{1-x}$ [17] nanowires with $x = 0.35$, $E_0(\infty)$ [10] is -0.5 eV.

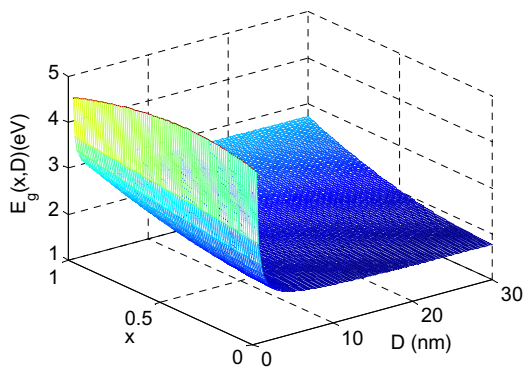


Fig. 5. Size dependence of composition-induced band-gap energy of $\text{Zn}_x\text{Cd}_{1-x}\text{Se}$ nanodots. The $E_0(\infty)$ [10] is -0.92 eV.

of band-gap of both the bulk and the nanometer scale with the size and the composition are similar, such as a downward bowing shape due to inter-atomic bond energy and a blue shift or red shift because of the band-gap intermixing of alloyed components. Consistency between theoretical predictions and experimental measurements of the II–VI semiconductor nanocompounds by altering composition implies that this model could be expected to be a general approach to analyze electrical and optical properties of nanosemiconductor system.

Acknowledgements

Project supported by the Major Research plan of the National Natural Science Foundation of China (Grant Nos. 10747129, 10772157 and 90606001), the National Fundamental Research Program of China (Grant No. 2007CB925204), the Natural Science Foundation of Hunan Province, China (Grant No. 07JJ3114) and Specialized Research Fund for the Doctoral Program of Higher Education of China (Grant No. 20050532013).

References

- [1] A.R. Clapp, I.L. Medintz, J.M. Mauro, B.R. Fisher, M.G. Bawendi, H. Mattoussi, *J. Am. Chem. Soc.* 126 (2004) 301.
- [2] M.J. Bowers, J.R. McBride, S.J. Rosenthal, *J. Am. Chem. Soc.* 127 (2005) 15378.
- [3] A. Rizzo et al., *Appl. Phys. Lett.* 90 (2007) 051106.
- [4] S. Kan, T. Mokari, E. Rothenberg, U. Banin, *Nature* 2 (2003) 155.
- [5] G. Ouyang, X.L. Li, X. Tan, G.W. Yang, *Appl. Phys. Lett.* 89 (2006) 031904.
- [6] C.Q. Sun, *Prog. Solid State Chem.* 35 (2007) 1.
- [7] R. Koole, G. Allan, C. Delerue, A. Meijerink, D. Vanmaekelergh, A.J. Houtepen, *Small* 4 (2008) 127.
- [8] X.Y. Lang, W.T. Zheng, Q. Jiang, *Nanotechnology* 7 (2008) 1536.
- [9] X. Zhong, Y. Feng, W. Knoll, M. Han, *J. Am. Chem. Soc.* 125 (2003) 13559.
- [10] Y.F. Zhu, X.Y. Lang, Q. Jiang, *Adv. Funct. Mater.* 18 (2008) 1422.
- [11] C.C. Yang, S. Li, *J. Phys. Chem. C* 112 (2008) 2851.
- [12] D.S. Sutraye, G.S. Shahane, V.B. Patil, L.P. Deshmukh, *Mater. Chem. Phys.* 65 (2000) 298.
- [13] A.H. Ammar, *Vacuum* 60 (2001) 355.
- [14] D.V. Petrov, B.S. Santos, G.A.L. Pereira, D.C. De Mello, *J. Phys. Chem. B* 106 (2002) 5325.
- [15] R.E. Bailey, S. Nie, *J. Am. Chem. Soc.* 125 (2003) 7100.
- [16] C.X. Shan, Z. Liu, C.M. Ng, S.K. Hark, *Appl. Phys. Lett.* 87 (2005) 033108.
- [17] Y. Liang, L. Zhai, X. Zhao, D. Xu, *J. Phys. Chem. B* 109 (2005) 7120.
- [18] Y. Li, H. Zhong, R. Li, Y. Zhou, C. Yang, *Adv. Funct. Mater.* 16 (2006) 1705.
- [19] L.A. Swafford et al., *J. Am. Chem. Soc.* 128 (2006) 12299.
- [20] J.P. Ge, S. Xu, J. Zhuang, X. Wang, Q. Peng, Y.D. Yi, *Inorg. Chem.* 45 (2006) 4922.
- [21] A. Pan et al., *J. Phys. Chem. B* 110 (2006) 22313.
- [22] G. Ouyang, C.Q. Sun, W.G. Zhu, *J. Phys. Chem. B* 112 (2008) 5027.
- [23] V.M. Goldschmidt, *Ber. Deut. Chem. Ges.* 60 (1927) 5027.
- [24] L. Pauling, *J. Am. Chem. Soc.* 60 (1927) 1270.
- [25] G. Ouyang, X. Tan, C.X. Wang, G.W. Yang, *Nanotechnology* 17 (2006) 4257.
- [26] L.H. Liang, D. Liu, Q. Jiang, *Nanotechnology* 14 (2003) 438.
- [27] M.C. Tamargo, *Optical Properties and Electronic Structure of Wide Band Gap II–VI Semiconductors*, New York, 2002, p. 113.
- [28] D. Denzler, M. Olschewski, K. Sattler, *J. Appl. Phys.* 84 (1998) 2841.
- [29] K.W. Kwak, R.D. King-Smith, D. Vanderbilt, *Phys. Rev. B* 48 (1993) 17827.
- [30] S.P. Mondal, K. Das, A. Dhar, S.K. Ray, *Nanotechnology* 18 (2007) 095606.
- [31] J. Hambrock, A. Birkner, R.A. Fischer, *J. Mater. Chem.* 11 (2001) 3197.
- [32] X. Ouyang, T.Y. Tsai, D.H. Chen, Q.J. Huang, W.H. Cheng, A. Clearfield, *Chem. Commun.* 7 (2003) 886.
- [33] N. Herron et al., *J. Am. Chem. Soc.* 111 (1989) 530.
- [34] A. Kasuya et al., *Nature* 3 (2004) 99.
- [35] Y. Nakaoka, Y. Nosaka, *Langmuir* 13 (1997) 708.
- [36] V.V. Nikesh, S. Mahamuni, *Semicond. Sci. Technol.* 16 (2001) 687.
- [37] D. Pan, Q. Wang, S. Jiang, X. Ji, L. An, *Adv. Mater.* 17 (2005) 176.